REPORT DOCUMENTATION PAGE

1. REPORT DATE (DD-MM-YYYY)	2. REPORT TYPE	3. DATES COVERED (From - To)
10-02-1998	Paper	

4. TITLE AND SUBTITLE	5a. CONTRACT NUMBER
Modeling of Interfacial Fracture in Incompressible Materials	5b. GRANT NUMBER
	5c. PROGRAM ELEMENT NUMBER

6. AUTHOR(S)	5d. PROJECT NUMBER
T.C. Miller	2302
	5e. TASK NUMBER
	M1G2
	5f. WORK UNIT NUMBER

7. PERFORMING ORGANIZATION NAME(S) AND ADDRESS(ES) AND ADDRESS(ES)	8. PERFORMING ORGANIZATION REPORT
Air Force Research Laboratory (AFMC) SPARTA 5 Pollux Drive Edwards AFB CA 93524-7048	

9. SPONSORING / MONITORING AGENCY NAME(S) AND ADDRESS(ES)	10. SPONSOR/MONITOR'S ACRONYM(S)
Air Force Research Laboratory (AFMC) AFRL/PRS 5 Pollux Drive Edwards AFB CA 93524-7048	11. SPONSOR/MONITOR'S NUMBER(S) AFRL-PR-ED-TP-1998-041

12. DISTRIBUTION / AVAILABILITY STATEMENT
Approved for public release; distribution unlimited.

13. SUPPLEMENTARY NOTES

14. ABSTRACT

20020115 079

15. SUBJECT TERMS

16. SECURITY CLASSIFICATION OF:			17. LIMITATION OF ABSTRACT	18. NUMBER OF PAGES	19a. NAME OF RESPONSIBLE PERSON C.T. Liu
a. REPORT Unclassified	b. ABSTRACT Unclassified	c. THIS PAGE Unclassified	A		19b. TELEPHONE NUMBER (include area code) (661) 275-5642

MODELING OF INTERFACIAL FRACTURE IN INCOMPRESSIBLE MATERIALS WITH VARYING MODULUS MISMATCH*

T. C. Miller

Sparta Incorporated

2 Draco Drive, Edwards Air Force Base, CA 93524

ABSTRACT

Numerical modeling is used to evaluate the effects of modulus mismatch on interfacial fracture. Different modulus ratios are considered, as are different mode mixities. The magnitudes of the complex stress intensity factors are evaluated using the energy domain integral approach, and the phase angles are measured using extrapolation of bond line traction data to r = 0. The results indicate that moderate changes in the modulus ratio have only a small effect on either the magnitude or phase angle of the complex stress intensity factor. These predictions confirm earlier experimental conclusions and suggest that the elastic mismatch is not a strong factor in determining the interfacial fracture of plane strain incompressible materials.

INTRODUCTION

The use of fracture mechanics to assess and predict crack development in solid propellants has led to cost savings by enabling better service life predictions for solid rocket motors. Both linear elastic and elastic-plastic fracture mechanics concepts have been used to predict crack propagation in solid propellants. A frequent site for the initiation and growth of cracks in solid rocket motors is the interface between the propellant and the rubber liner. This study examines this situation, namely, that of an interfacial crack lying between two incompressible materials and subjected to plane strain.

A previous experimental work examined a similar situation.[1] Both homogeneous and bimaterial specimens were considered. In bimaterial specimens, the elastic moduli of the two materials differed by a factor of two. Additional results also indicated that larger differences between the two elastic moduli had little effect on the complex stress intensity factor.

The modulus ratio, E_2/E_1, depends on the materials used in the motor, and different values need to be considered. Typically, the stiffness of the propellant will exceed that of the liner by a factor of about 3. If it can be established that this ratio only weakly affects the complex stress intensity factor, then computations for interfacial cracking of different motors can be combined in a simplified analysis. The present work uses numerical methods to vary E_2/E_2 from 1 to 6 to study this issue.

DISCUSSION

FIELD EXPRESSIONS

Figure 1 shows a crack and corresponding coordinate system lying along an interface between two distinct linear elastic isotropic materials. If the materials are both incompressible and plane strain conditions exist, then the bimaterial parameter, ε, normally associated with interfacial cracks, vanishes. This is a degenerate case of the more general interfacial cracking problem and it has field expressions that closely resemble those of cracks in homogenous bodies subjected to mixed mode loading. One consequence of the vanishing of ε is that both the

---

phase angle (Ψ) of the complex stress intensity factor (**K**)[*] and the ratio of stress components σ_{xy} and σ_{yy} along the bond line are invariant with respect to distance from the crack tip and are related:[2]

$$(\sigma_{yy} + i\sigma_{xy})_{\theta=0} = \frac{K}{\sqrt{2\pi r}} = \frac{Ke^{i\Psi}}{\sqrt{2\pi r}} \tag{1}$$

Here **K** is the complex stress intensity factor, and can be expressed in either rectangular or polar form (i.e., $K = K_I + K_{II} = Ke^{i\Psi}$). This expression holds in the near tip or asymptotic region, where the term with the $r^{-1/2}$ singularity eclipses the other terms in the Williams expansion.

Also, J, the contour integral, and K, the magnitude of the complex stress intensity factor, are related through an effective plane strain modulus:

$$J = \frac{K^2}{\overline{E}^*}$$

$$\frac{1}{\overline{E}^*} = \frac{1}{2}\left[\frac{1}{\overline{E}_1} + \frac{1}{\overline{E}_2}\right] \tag{2}$$

$$\overline{E}_1 = \frac{E_1}{1-\nu_1^2}, \quad \overline{E}_2 = \frac{E_2}{1-\nu_2^2}$$

Because $\nu_1 = \nu_2 = 1/2$ for incompressible materials, additional simplifications could be made. More general expressions for stress and displacement components in the near tip region have been derived[2], but for this work only eqs. (1) and (2) are needed.

NUMERICAL MODELS

A typical finite element model is shown in Fig. 2. The geometry of the numerical models simulates the experimental specimens from the related photoelastic study. The specimens are glued to aluminum grips, which are free to rotate when loaded. Mode mixity is varied by changing the crack orientation with respect to the mode I loading direction. When the crack is oriented horizontally, mode I loading takes place and $K_{II} = 0$. However, as the crack orientation angle α varies, the mode II component becomes increasingly significant. Crack orientation angles of 0°, 15°, 30°, and 45° were studied in both the experimental and numerical work so that fracture under different mode mixities could be studied (the corresponding mode mixities vary from about 0° to 30°). The numerical models also allow for a range of modulus ratios: $E_2/E_1 = 1$ (a homogeneous specimen), as well as $E_2/E_1 = 2$, 4, and 6.

One other noteworthy aspect of the models is the use of hybrid elements. The use of incompressible materials in plane strain causes an indeterminacy due to a vanishing of a term (1-2ν) that appears in the constitutive equations. This results in a singular global stiffness matrix. The problem is resolved by using a hybrid formulation. In this formulation, the hydrostatic portion of the stress tensor is used as a solution variable in addition to the components of nodal displacements.[3,4]

[*]Throughout the text, boldface type is used to indicate that a symbol represents either a complex or vector quantity.

DETERMINING FRACTURE PARAMETERS FROM NUMERICAL DATA

The primary results from the finite element analysis are the nodal displacements. Secondary results such as stress components are obtainable with derivatives of shape functions, material properties, and nodal displacements. The displacements, stresses, and strains are used to determine both the magnitude and phase angle of the complex stress intensity factor, K. Evaluation of the phase angle, Ψ, is accomplished using eq. (1). As this equation shows, $\tan^{-1}(\sigma_{xy}/\sigma_{yy})$ along $\theta = 0°$ and inside the near tip zone is equal Ψ. The value of Ψ can be estimated from stress data by evaluating σ_{xy} and σ_{yy} along part of the bond line near the crack tip and fitting a polynomial curve to the data so that $\tan^{-1}(\sigma_{xy}/\sigma_{yy})$ is a function of r. The constant term of this polynomial corresponds to $\tan^{-1}(\sigma_{xy}/\sigma_{yy})$ at $r = 0$, and is an estimate of Ψ.

This regression method has been used previously with similar numerical models and compared with corresponding experimental data with good results.[5] Linear elasticity requires that σ_{yy} and σ_{xy} be continuous across the bond line, but there is not exact continuity in the finite element results because of their approximate nature. In practice, the stresses at a node on an element are extrapolated from the Gaussian integration point values. Then, for stresses at nodes on the bond line, the mean of the results for each element is determined for use with the regression analysis.

Equation (2) is used to determine K, the magnitude of the complex stress intensity factor, by first evaluating J. The parameter J is found because of its ease of evaluation in numerical models and because of its robust nature. In this work, J is evaluated using the domain integral method, which uses the Gauss divergence theorem to convert the contour integral to an equivalent area integral. The area integral is then found using results for the field variables of the elements that the area contains. The value of K is then found using eq. (2). Previous experience with this method of determining K has also indicated good agreement with existing experimental data.[5,6]

RESULTS

Crack orientations of 0°, 15°, 30°, and 45° were considered. Elastic modulus ratios of 1, 2, 4, and 6 were used to test the effects of relative stiffness. The top portions of the specimens always have E = 2698 psi (18.60 MPa), corresponding to the stiffness of a photoelastic polymer used in related experimental work. The moduli of the lower portion of the specimens were varied to change the modulus ratio. Loads of 5.25 lbs. (23.4 N) were applied to the aluminum grips, giving a nominal stress of 7.00 psi (48.3 kPa).

Figure 3 shows the variation in K with E_2/E_1 for all crack orientations. As E_2/E_1 is varied from 1 to 2, elevations in K of 15-17% occur. However, changes in E_2/E_1 above this level have little effect on K. Similarly, Fig. 4 shows the variation in Ψ, the phase angle of K. As E_2/E_1 changes from 1 to 2, Ψ changes by 4° in the worst case (i.e., for a crack orientation of 0°). Variations in the phase angle are smaller as E_2/E_1 changes from 2 to 6.

The results suggest that for elastic modulus ratios from 2 to 6, the value of both the magnitude and phase angle of K vary only weakly, so that K depends on the remote applied load, the orientation of the load relative to the interface, and the crack length. This is important because propellant material properties such as modulus vary among propellants, and vary significantly even for identical formulations. Because the propellant is a mixed particulate composite, homogeneity of the cured cylinders is difficult, causing differences in the material composition within cylinders of propellant. Also, differences in the material properties may occur near the interface due to diffusion of the two materials during the manufacturing process.

The primary reason for the weakness of the E_2/E_1 effect is that the modulus mismatch causes large changes in σ_{xx} only, with only small changes in σ_{xy} and σ_{yy}. This is shown in Figs. 5-7, which show the stress components for a specimen for the four different E_2/E_1 values tested. In the absence of a crack, the mismatch causes a differential contraction of the two materials as the specimen is loaded, giving σ_{xx} values that are tensile in the more compliant material and compressive in the stiffer material. This effect is shown in Fig. 8, which plots σ_{xx} vs. y as the bond line is traversed for a specimen with $E_2/E_1 = 6$. The data is taken from a cracked

specimen, but from a part of the specimen that is away from the specimen boundaries and from the crack tip. Near the crack tip, this differential contraction field is superimposed on the stress fields for the crack tip. The σ_{xx} values thus change substantially with E_2/E_1, whereas σ_{xy} and σ_{yy} do not.

Since Ψ relates to σ_{yy}/σ_{xy} in the near tip region, σ_{xx} does not affect Ψ. Changes effected in Ψ by altering relative stiffness are induced by small changes in shear stresses in the near tip region. A similar effect occurs with the magnitude K or with the value of J (since they are related through eq. (2)). Here, σ_{xx} is a traction component along the contour that defines J, with the σ_{xx} contribution due to differential contraction being a function of y. This traction component makes equal but opposite contributions to different parts of the contour, so that no net increase in J is produced.

SUMMARY AND CONCLUSIONS

Cracks along interfaces between incompressible materials under plane strain conditions exist in solid rocket motors and have a bimaterial parameter $\epsilon = 0$, which simplifies the field expressions for the cracks. The phase angle of the complex stress intensity factor can be determined from numerical results using bond line traction data. The magnitude of the complex stress intensity factor can be determined using J integral determinations. For a variety of mode mixities, it was found that neither the magnitude nor the phase angle varied significantly as the modulus ratio for the material combinations varied from 2 to 6. More substantial changes took place as the modulus ratio was varied from 1 to 2. For most combinations of propellant and liner used in solid rocket motors, the magnitude and phase angle of K are functions of loading, geometry, and crack length, and are not strongly influenced by the relative stiffness of the propellant and liner.

LIST OF SYMBOLS

E	Young's modulus
J	J integral value
K	magnitude of the complex stress intensity factor
K	complex stress intensity factor
ϵ	bimaterial parameter
ν	Poisson's ratio
σ_{xx} , σ_{xy} , σ_{yy}	in-plane stress components
Ψ	phase angle of the complex stress intensity factor

REFERENCES

1. Smith, C. W., Finlayson, E. F., and Liu, C. T., "A Method for Evaluating Stress Intensity Distribution for Cracks in Rocket Motor Bondline," Engineering Fracture Mechanics (to be published).

2. Hutchinson, J. W., and Suo, Z., "Mixed Mode Cracking in Layered Materials," Advances in Applied Mechanics, Vol. 29, Academic Press, 63-91 (1992).

3. ABAQUS/Standard User's Manual, Version 5.5, Vol. 1, Hibbitt, Karlsson, and Sorenson, Pawtucket, RI (1995).

4. ABAQUS Theory Manual, Version 5.5, Vol. 1, Hibbitt, Karlsson, and Sorenson, Pawtucket, RI (1995).

5. Miller, T. C., Modeling of Interfacial Fracture in Photoelastic Specimens, Proceedings of the 1998 Society

for Experimental Mechanics Spring Conference, Houston, TX (to be published).

6. Miller, T. C., and Chona, R., An Experimental Investigation of a Thermally Loaded Interfacial Crack, Proceedings of the 1997 Society for Experimental Mechanics Spring Conference, Bellevue, WA (1997).
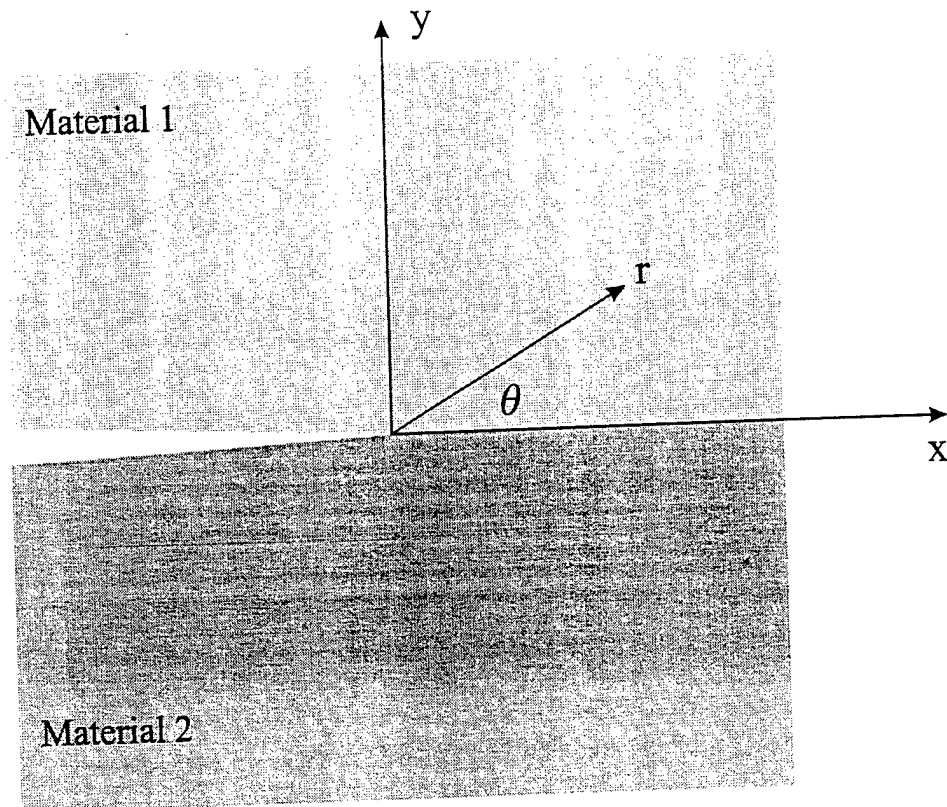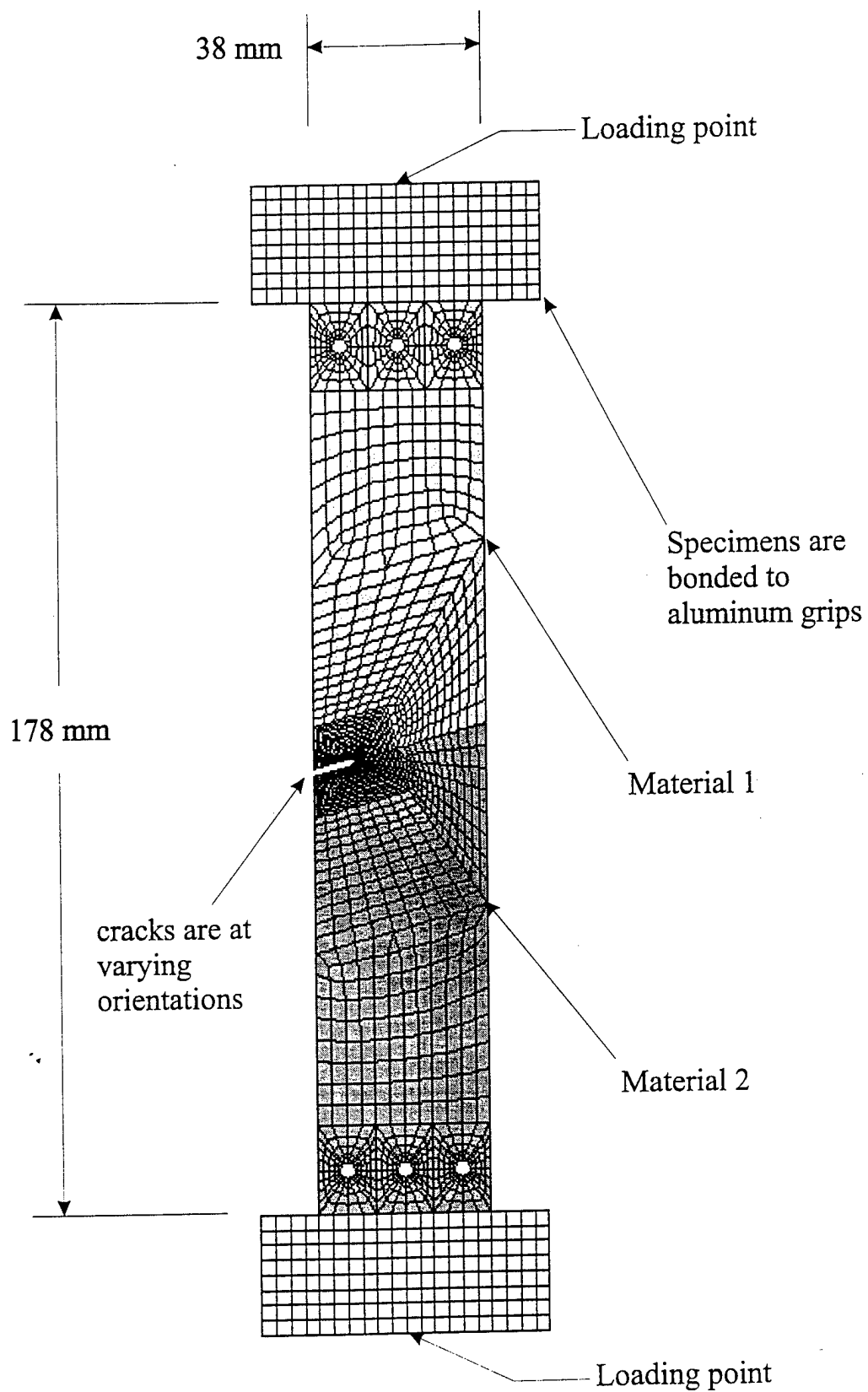
Fig. 1 — Geometry of an Interfacial Crack

38 mm

Loading point

Specimens are
bonded to
aluminum grips

Material 1

178 mm

cracks are at
varying
orientations

Material 2

Loading point

Fig. 2 - Typical Finite Element Model for a Bimaterial Specimen

crack orientation [deg.]
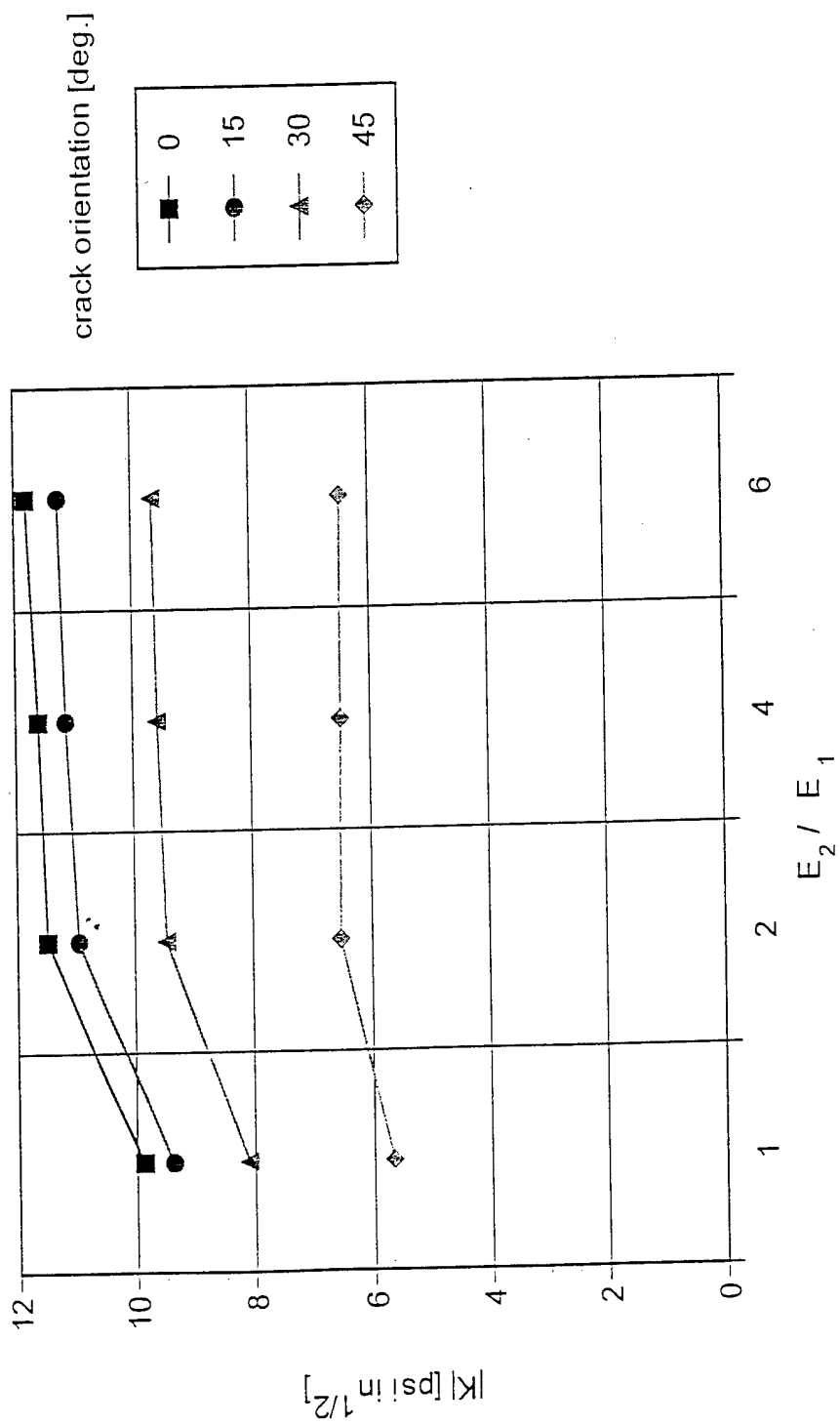
- ■ 0
- ● 15
- ▲ 30
- ◈ 45

$|K| \; [psi \; in^{1/2}]$

$E_2 \; / \; E_1$

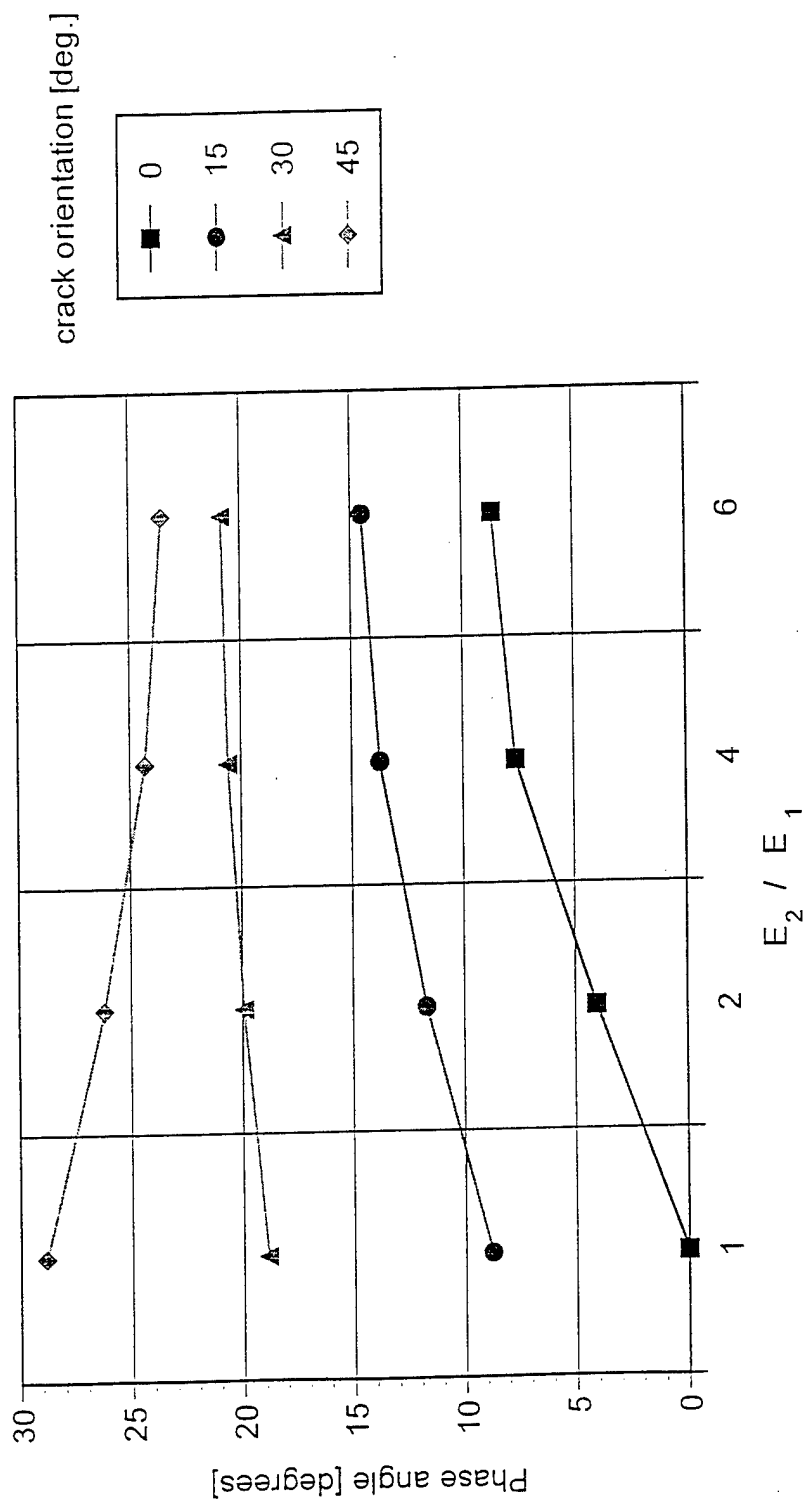Fig. 3 – Variation of Stress Intensity Factor Magnitude
with Modulus Ratio

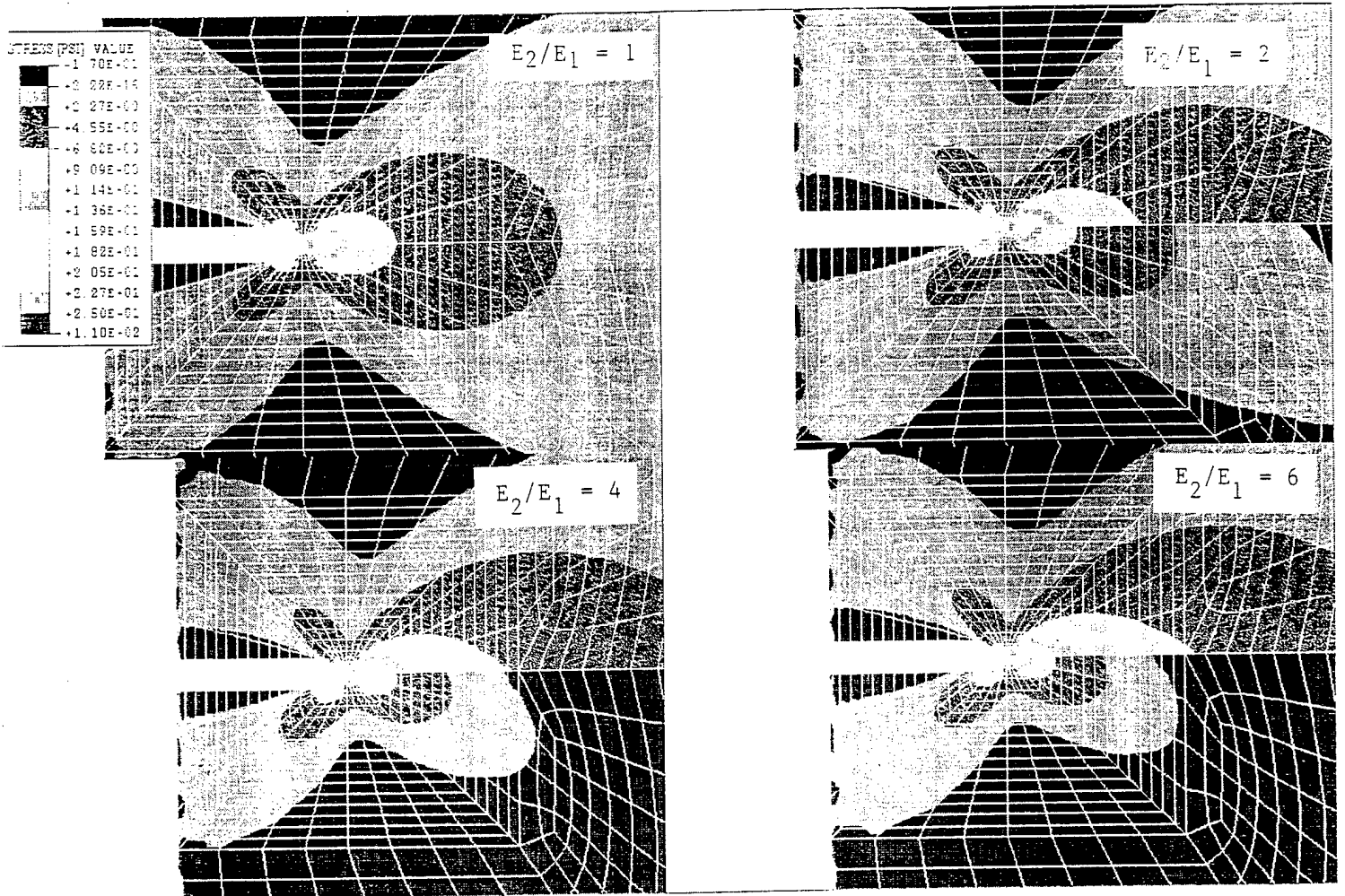Fig. 4 – Variation of Stress Intensity Factor Phase Angle with Modulus Ratio

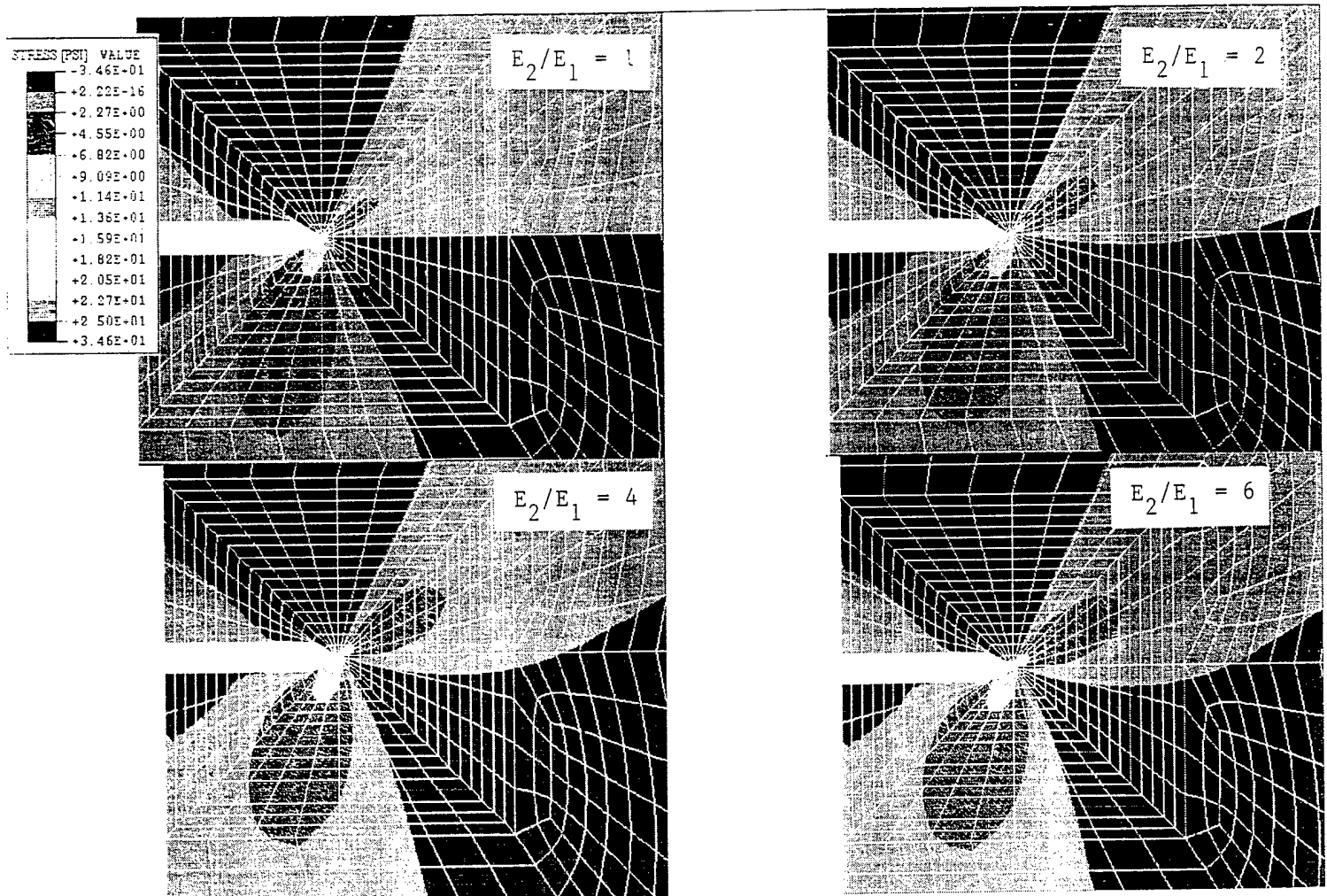Fig. 5 – Contour Plots of σ_{xx} with Different Modulus Ratios

STRESS [PSI] VALUE
-3.46E+01
+2.22E-16
+2.27E+00
+4.55E+00
+6.82E+00
+9.09E+00
+1.14E+01
+1.36E+01
+1.59E+01
+1.82E+01
+2.05E+01
+2.27E+01
+2.50E+01
+3.46E+01

$E_2/E_1 = 1$

$E_2/E_1 = 2$

$E_2/E_1 = 4$

$E_2/E_1 = 6$

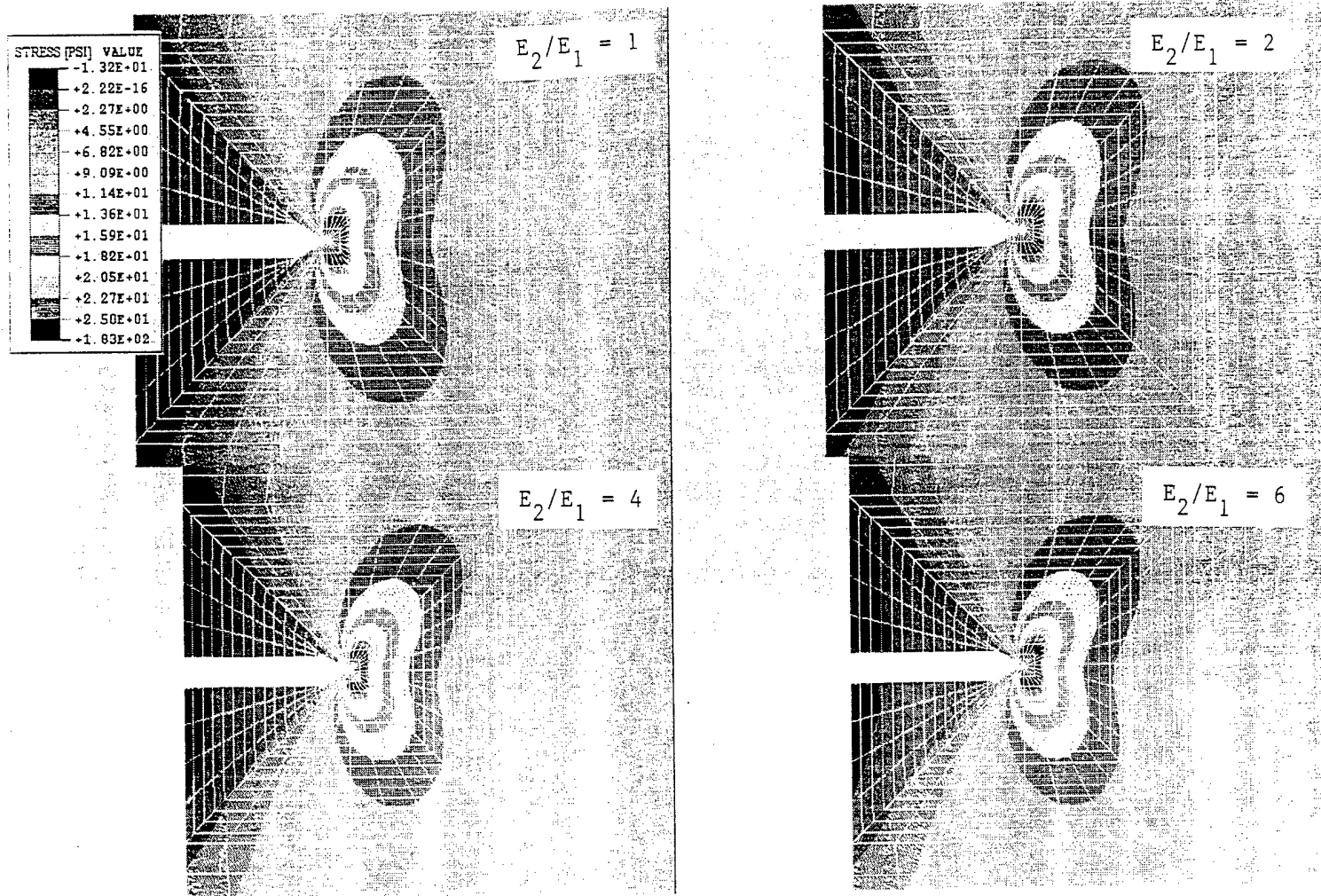Fig. 6 – Contour Plots of σ_{xy} with Different Modulus Ratios

Fig. 7 – Contour Plots of σ_{yy} with Different Modulus Ratios